

# Optical investigation of the charge-density-wave phase transitions in $\text{NbSe}_3$

A. Penucci<sup>1</sup>, L. Degiorgi<sup>2,1</sup>, and R.E. Thome<sup>3</sup>

<sup>1</sup>Laboratorium für Festkörperphysik,

ETH Zurich, CH-8093 Zurich, Switzerland

<sup>2</sup>Paul Scherrer Institute, CH-5232 Villigen and

<sup>3</sup>Department of Physics, Cornell University, Ithaca NY 14853, U.S.A.

(Dated: March 22, 2024)

## Abstract

We have measured the optical reactivity  $R(\omega)$  of the quasi one-dimensional conductor  $\text{NbSe}_3$  from the far infrared up to the ultraviolet between 10 and 300 K using light polarized along and normal to the chain axis. We find a depletion of the optical conductivity with decreasing temperature for both polarizations in the mid to far-infrared region. This leads to a redistribution of spectral weight from low to high energies due to partial gapping of the Fermi surface below the charge-density-wave transitions at 145 K and 59 K. We deduce the bulk magnitudes of the CDW gaps and discuss the scattering of ungapped free charge carriers and the role of fluctuations etc.

PACS numbers: 78.20.-e, 71.30.+h, 71.45.Lr

When metals are cooled, they often undergo a phase transition to a state characterized by a new type of order. Of particular interest are the quasi-one-dimensional linear-chain metals because they exhibit important deviations from Fermi liquid behaviour and unusual phenomena associated with charge- and spin-density-wave broken symmetry ground states<sup>1,2</sup>. A charge-density-wave (CDW) is a condensate comprised of a coupled modulation of the conduction electron density and lattice atom positions. It forms via a Peierls transition, in which an instability of the metallic Fermi surface (FS) due to nesting at  $q = 2k_F$  ( $k_F$  being the Fermi wave-vector) couples to the Kohn anomaly in the phonon spectrum<sup>3,4,5</sup>. As in conventional superconductivity the electron-phonon coupling is the dominant interaction<sup>1</sup>, and the transition leads to opening of a charge gap.

The transition metal trichalcogenides  $MX_3$  with  $M = Nb; Ta; Ti$  and  $X = S; Se; Te$  are among the most interesting materials displaying low dimensional electronic properties. Their crystallographic structure is made up of infinite chains of trigonal prisms<sup>1</sup>. Depending on the coupling between chains, they can exhibit pseudo-gap one-dimensionality to anisotropic three dimensionality. The most remarkable properties have been observed in  $NbSe_3$ , which shows the phenomena of density wave transport cleanly than any other known system<sup>1</sup>. The resistivity remains metallic down to low temperatures, but two CDW phase transitions occur at  $T_1 = 145$  K and  $T_2 = 59$  K where the resistivity shows a sharp increase<sup>6</sup>. Tight binding calculations<sup>7</sup> have shown that  $NbSe_3$  has a primarily one-dimensional character with deviations due to the short intra- and interlayer Se-Se contacts. This transverse coupling produces a warped Fermi surface so that imperfect nesting and only partial gapping are expected.

The transition at  $T_1$  is associated with a linear nesting, the wavevector of the CDW condensate pointing along the main chain axis, and the one at  $T_2$  with a diagonal nesting<sup>8</sup>. The literature values for the energy gaps, obtained by surface-sensitive techniques including point-contact, tunneling and angle resolved photoemission (ARPES) spectroscopies<sup>9,10,11,12,13</sup>, vary significantly:  $2_{T_1} = 110 - 220$  meV for the  $T_1$  CDW, and  $2_{T_2} = 40 - 90$  meV for the  $T_2$  CDW. In all cases the gap values yield a ratio  $2_{T_1} = k_B T_1$  much larger than the mean-field value of 3.52, and the mean-field transition temperature  $T_{MF}$  is much larger than the measured  $T_1$  and  $T_2$ . These discrepancies from mean-field values indicate the importance of one-dimensional fluctuations.

In principle, optical spectroscopic methods are an ideal bulk-sensitive tool in order to

investigate the CDW phase transitions<sup>1</sup>. Previous optical spectroscopy measurements were performed at room temperature<sup>14</sup> or over an insufficient energy range<sup>15,16</sup> which led to an erroneous evaluation of the CDW gaps. We provide here the first comprehensive study of the optical properties of NbSe<sub>3</sub> over a broad spectral range and as a function of temperature. The optical conductivity shows a redistribution of spectral weight from low to high frequencies with decreasing temperature, which we use to determine the bulk CDW (pseudo)gaps. We also observe precursor effects of the CDW phase transitions and establish that the resistivity anomalies are primarily the consequence of a Fermi surface gapping and not due to changes in the lifetime of the charge carriers.

High purity samples were grown as previously described<sup>17</sup>. This study was made possible by preparing aligned mosaic specimens consisting of several wide, flat NbSe<sub>3</sub> ribbons with a resulting optical surface 3 mm long by 2 mm wide. The optical reflectivity  $R(\omega)$  was measured from the far infrared up to the ultraviolet between  $T = 300$  K and 10 K. Polarizations along and transverse to the chain axis, corresponding to the b and c crystallographic axes, respectively, were used to assess the anisotropic electrodynamic response. The specimens were then coated with a 3000 Å gold layer and measured again, allowing correction for surface scattering from our mosaic samples without altering the overall shape and features of the spectra. Additional experimental details are described elsewhere<sup>2,18</sup>. Kramers-Kronig transformations were used to calculate the real part  $\sigma_1(\omega)$  of the optical conductivity. Standard high frequency extrapolations  $R(\omega) \propto \omega^{-s}$  (with  $2 < s < 4$ ) were employed<sup>18</sup> in order to extend the data set above  $10^5$  cm<sup>-1</sup> and into the electronic continuum. Because of scatter in the data at low frequencies (below 50 cm<sup>-1</sup>),  $R(\omega)$  was extrapolated using the Hagen-Rubens (HR) law  $R(\omega) = 1 - 2 \frac{P}{\omega} (\omega = \omega_{dc})$  from data points in the 30 to 70 cm<sup>-1</sup> range. This extrapolation yielded  $\omega_{dc}$  values in agreement with dc transport data<sup>6,19</sup>, providing further confirmation of the reliability of the gold-coating-corrected data. The temperature dependence of  $\sigma_1(\omega)$  is not affected by the details of this low frequency extrapolation.

Figure 1 shows the optical reflectivity at two selected temperatures. It is metallic at all temperatures and for both polarization directions, but there is a remarkable anisotropy between the two crystallographic directions. For light polarized along the b-axis the  $R(\omega)$  plasma edge has a sharp onset around 1 eV ( $\approx 8000$  cm<sup>-1</sup>), while along the c-axis a much more gradual and broad onset begins at about 0.5 eV ( $\approx 4000$  cm<sup>-1</sup>).  $R(\omega)$  along the c-axis resembles the so-called overdamped behaviour<sup>18</sup> typically seen in low dimensional systems<sup>2</sup>

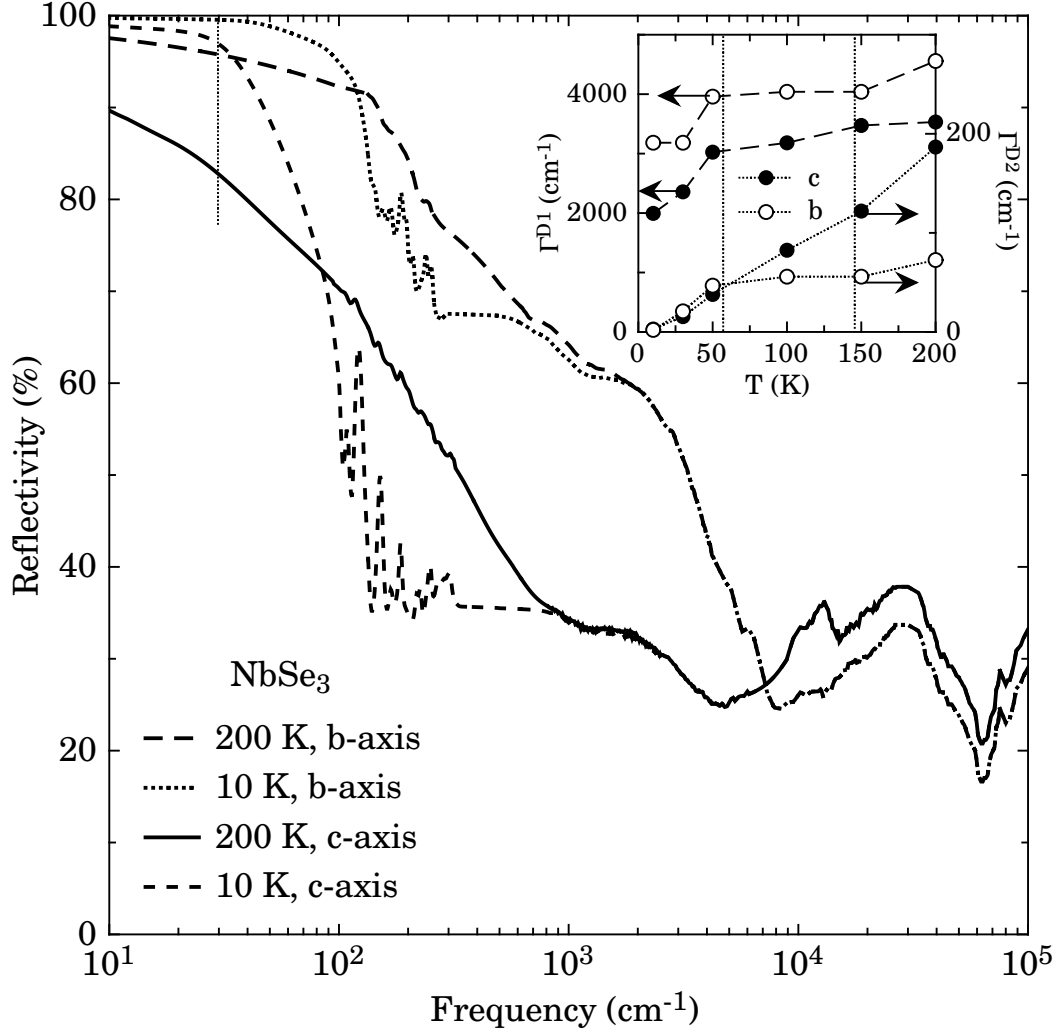


FIG. 1: Optical reflectivity  $R(\omega)$  in  $\text{NbSe}_3$  along both polarization directions and at two selected temperatures (10 and 200 K). The thin dotted line marks the frequency below which the Hagen-Rubens extrapolation has been performed. The inset shows the temperature dependence of the scattering rates for the first ( $\Gamma_{D1}$ , left y-axis scale) and second ( $\Gamma_{D2}$ , right y-axis scale) Drude term in the fits to both polarization directions. Solid symbols refer to the c-axis and open ones to the b-axis. The CDW transition temperatures are indicated by thin dotted lines.

and may indicate incoherent charge transport along the c direction. Previous  $R(\omega)$  data<sup>14</sup> at 300 K and over a smaller spectral range also showed anisotropic behaviour. At low temperatures,  $R(\omega)$  for both polarizations is depleted in the far and mid-infrared spectral range, but both show a sharp upturn at low frequencies. This upturn leads to a crossing of the 200 K and 10 K spectra around  $100 \text{ cm}^{-1}$  (well within the measured spectral range in

Fig. 1) so that  $R(\omega)$  increases with decreasing temperatures in the  $\omega \rightarrow 0$  limit. Our 10 K data for light polarized along the b-axis bear some similarities with earlier results at 2 K of Challaner and Richard<sup>15</sup> which only covered the far infrared range ( $\omega < 400 \text{ cm}^{-1}$ ).

Figure 2 shows the temperature dependence of the excitation spectrum below  $4000 \text{ cm}^{-1}$  as revealed by the real part  $\epsilon_1(\omega)$  of the optical conductivity. Above  $4000 \text{ cm}^{-1}$  several absorptions (not shown here) ascribed to electronic interband transitions<sup>14</sup> are observed. In the infrared spectral range,  $\epsilon_1(\omega)$  for both polarizations shows a rather strong mid-infrared band at  $2000 \text{ cm}^{-1}$  along the b-axis and at  $3000 \text{ cm}^{-1}$  along the c-axis. The low frequency sides of the absorptions for both the b and c axes have broad shoulders located below about  $1000 \text{ cm}^{-1}$ . There is an obvious suppression of spectral weight in the infrared range with decreasing temperature, while the effective (Drude) metallic component in the far infrared shifts to lower frequency and narrows. The narrowing of  $\epsilon_1(\omega)$  at low frequencies and temperatures follows from the steep increase of  $R(\omega)$  around  $100 \text{ cm}^{-1}$  in Fig. 1. At low temperatures the narrowing is so strong that the spectral weight of the effective (Drude) metallic component falls entirely below our data's low-frequency limit. This leads to an apparent disagreement in Fig. 2 between  $\epsilon_1(\omega \rightarrow 0)$  and  $\epsilon_{dc}$ , which results from the HR extrapolation used for  $R(\omega)$  below  $50 \text{ cm}^{-1}$ .

In order to better highlight the relevant energy scales characterizing the excitation spectrum and in particular to address the redistribution of spectral weight versus temperature in  $\epsilon_1(\omega)$  and its connections with the CDW transitions in  $\text{NbSe}_3$ , we have applied the phenomenological Lorentz-Drude (LD) approach based on the classical dispersion theory<sup>18</sup>. For both polarization directions, the high-frequency response is fitted using Lorentz harmonic oscillators to describe the high-frequency electronic interband transitions. The low-frequency response can be fitted with two Drude terms and two mid-infrared harmonic oscillators at about  $561$  and  $2270 \text{ cm}^{-1}$  for the b-axis and at about  $1100$  and  $2920 \text{ cm}^{-1}$  for the c-axis (inset of Fig. 2). The two Drude terms could represent two conduction bands<sup>19</sup> that are both affected by the CDW transitions. Sharp Lorentz harmonic oscillators are used to fit the IR-active phonon modes which appear with decreasing temperature<sup>15</sup>. These modes contribute only a tiny fraction of the spectral weight below  $100 \text{ K}$  in agreement with a previous infrared study of  $\text{NbSe}_3$  (Ref. 15), and are likely phasons<sup>20,21</sup> arising from the coupling between the lattice and the CDW condensate. With this minimum set of Lorentz and Drude terms, we obtain an outstanding fit to  $\epsilon_1(\omega)$  at all temperatures<sup>22</sup>.

Figure 3 shows how the spectral weight is redistributed among the Drude and mid-infrared Lorentz terms as temperature decreases. Both Drude terms lose spectral weight (i.e., the corresponding plasma frequency decreases) with decreasing temperature, with a more pronounced loss occurring below 100 K. The suppressed Drude weight is transferred to high energies and in particular to the mid-infrared absorptions, for both polarization directions. Along the b-axis the harmonic oscillator at  $2270 \text{ cm}^{-1}$  acquires most of the transferred weight, while along the c-axis both absorptions gain weight. Part of the c-axis weight is transferred to even higher energies and into the electronic continuum. Nevertheless, the total spectral weight  $\int_0^{\infty} \epsilon_1(\omega) d\omega$  for both polarization directions is fully recovered by  $10^4 \text{ cm}^{-1}$  ( $\sim 1 \text{ eV}$ ), satisfying the optical sum rule. In this regard NbSe<sub>3</sub> closely resembles the 2H-XSe<sub>2</sub> dichalcogenides<sup>23</sup>, and does not show the "sum rule violation" of the high-temperature superconductors since the nature of the correlations in the two ground states are different<sup>23,24</sup>.

The depletion of the Drude spectral weight in  $\epsilon_1(\omega)$  with decreasing temperature indicates a progressive gapping of the Fermi surface, which gets partially destroyed at the Peierls transitions. The inset of Fig. 3a shows the fraction change of the total Drude weight for both the b and c directions as a function of temperature. Ong and Monceau<sup>6</sup> estimated from transport data that approximately 20% of FS is destroyed at  $T_1$ , while 62% of the remaining 80% is destroyed by gaps at  $T_2$ . The corresponding values of residual ungapped Fermi surface are marked by dashed lines in the inset to Fig. 3a, and are in excellent agreement with the present results for the b-axis. We attribute the harmonic oscillator at  $2270 \text{ cm}^{-1}$  (281 meV) to the  $T_1$  CDW gap<sup>25</sup> associated with linear nesting along the chain b-axis, and the oscillator at  $561 \text{ cm}^{-1}$  (70 meV) to the  $T_2$  CDW gap associated with the diagonal nesting<sup>8,12</sup>. In c-axis data, the CDW gap due to linear nesting should not be observable in our spectra (i.e., the transition probability is zero), so we attribute the harmonic oscillator at  $1100 \text{ cm}^{-1}$  (136 meV) to the CDW gap associated with the diagonal nesting. This suggests anisotropic gapping for the diagonal nesting<sup>13</sup>. The optical gaps compare well with the broad interval of gap estimates from tunneling, point-contact and ARPES spectroscopy<sup>9,10,11,12,13</sup>. Our estimated (direct) optical CDW gaps are larger than the indirect gaps obtained from tunneling<sup>9,10,11</sup>. Deviations from the k-resolved ARPES findings<sup>8,12</sup> may arise in part because optical measurements average over the k-space. Additional deviations may result because of differences between the bulk optical value and the near-surface value probed by these other

techniques. Our gap value for the  $T_2$  CDW transition and for light polarized along  $b$  is a factor of three to four larger than the estimate<sup>15</sup> of  $120\text{--}190\text{ cm}^{-1}$  ( $15\text{--}24\text{ meV}$ ) obtained in the first and only other optical study at low temperature of  $\text{NbSe}_3$ . At the time of these earlier measurements the large ratio  $2/k_B T$  characteristic of these materials was not recognized, and so data collection did not extend much beyond energies corresponding to the measured  $T_2$  and the mean-field ratio. Our  $c$ -axis  $\epsilon_1(\omega)$  data and LD analysis indicate the presence of another absorption at about  $2920\text{ cm}^{-1}$  ( $362\text{ meV}$ ). This energy is too large to be ascribed to a CDW gap<sup>9,10,11,12,13,14,15</sup>, and likely arises from the band structure. It may be a hybridization-like gap induced by Brillouin zone backfolding arising from the Fermi surface nesting<sup>8</sup>.

The  $b$  and  $c$  axis absorptions at  $561$  and  $1100\text{ cm}^{-1}$ , respectively (thin dotted lines in Fig. 2), slightly soften with increasing temperature. However, the mid-infrared absorptions persist to temperatures well above  $T_1$  and  $T_2$ . This provides evidence for the importance of 1D fluctuations<sup>26</sup> in the regime between the measured transition temperatures and the much larger  $T_{MF}$ . Evidence for these fluctuations has previously been obtained in X-ray diffraction<sup>4</sup>, ARPES<sup>8,12</sup>, and tunneling experiments<sup>10</sup>. In light of these strong fluctuation effects, the mean-field or BCS-like form of the temperature dependence of the CDW gap observed in X-ray diffraction<sup>5</sup> and point-contact spectroscopy experiments<sup>13</sup> remains puzzling.

Finally, we comment on the temperature dependence of the scattering rates  $(\gamma)$  for the Drude terms, shown in the inset of Fig. 1. The  $\gamma$  value for the first (narrow) Drude term is partially determined by the HR extrapolation of  $R(\omega)$ . However, its temperature dependence is strikingly similar to that of  $\gamma$  for the second (broad) Drude term, which covers an extended spectral range going well beyond the range of the HR extrapolation, suggesting that the extrapolation is not responsible for the observed behavior. As directly indicated by the narrowing of  $\epsilon_1(\omega)$  with decreasing temperature, the scattering rates show a pronounced drop below  $50\text{ K}$  for both Drude terms and both polarization directions. As in the two-dimensional  $2\text{H-NbSe}_2$  dichalcogenide system<sup>23</sup> this clearly indicates that some scattering channels freeze out when the long-range-ordered CDW condensate develops. On the other hand, short range ordered CDW segments present for temperatures  $T > T_2$  can lead to additional scattering of the ungapped charge carriers. The weak temperature dependence of  $\gamma$  above  $T_2$  reinforces the notion<sup>19</sup> that the (CDW) resistivity anomalies are due to changes in the carrier concentration (inset of Fig. 3a) and not in the lifetime.

In conclusion, we have performed the first complete and bulk sensitive optical investigation of  $\text{NbSe}_3$ , the most important CDW system to show collective transport. We identify the energy scales associated with the CDW gaps, determine the fractional gapping of the Fermi surface, observe CDW fluctuation effects above the experimental Peierls transitions, and establish the suppression of the free charge carriers scattering in the broken symmetry ground state.

#### Acknowledgments

The authors wish to thank J. Müller for technical help, and R. Claessen, J. Schaffer and M. G. Rioni for fruitful discussions. This work has been supported by the Swiss National Foundation for the Scientific Research and by the NSF (DMR-0101574).

- 
- <sup>1</sup> G. G. Gurun, in *Density waves in solids*, (Addison Wesley, 1994) and references therein.
  - <sup>2</sup> V. Vescoli et al., *Eur. Phys. J. B* **13**, 503 (2000).
  - <sup>3</sup> J. P. Pouget and R. Comes, in *Charge Density Waves in Solids*, L. P. Gor'kov, G. G. Gurun, eds., North Holland, Amsterdam (1989), p. 85.
  - <sup>4</sup> A. H. Moudouen et al., *Phys. Rev. Lett.* **65**, 223 (1990); S. Rouziere et al., *Solid State Commun.* **97**, 1073 (1996).
  - <sup>5</sup> R. M. Fleming et al., *Phys. Rev. B* **18**, 5560 (1978).
  - <sup>6</sup> N. P. Ong and P. Monceau, *Phys. Rev. B* **16**, 3443 (1977).
  - <sup>7</sup> E. Canadell et al., *Inorg. Chem.* **29**, 1401 (1990).
  - <sup>8</sup> J. Schaffer et al., *Phys. Rev. Lett.* **87**, 196403 (2001).
  - <sup>9</sup> T. Ekino and J. Akimitsu, *Physica B* **194-196**, 1221 (1994).
  - <sup>10</sup> Z. Dai et al., *Phys. Rev. Lett.* **66**, 1318 (1991) and H. Haifeng and Z. Dianlin, *Phys. Rev. Lett.* **82**, 811 (1999).
  - <sup>11</sup> A. Fournelle et al., *Phys. Rev. Lett.* **57**, 2199 (1986).
  - <sup>12</sup> J. Schaffer et al., *Phys. Rev. Lett.* **91**, 066401 (2003).
  - <sup>13</sup> A. A. Sinchenko and P. Monceau, *Phys. Rev. B* **67**, 125117 (2003).
  - <sup>14</sup> H. P. Gessrich et al., *Physica B* **143**, 174 (1986) and *Solid State Commun.* **49**, 335 (1984).



- <sup>15</sup> W .A .Challaner and P .L .Richard, Solid State Commun. 52, 117 (1984).
- <sup>16</sup> J.Nakahara et al., J.Phys.Soc.Jpn. 54, 2741 (1985).
- <sup>17</sup> R.E.Thorne, Phys.Rev.B 45, 5804 (1992).
- <sup>18</sup> F.Wooten, in Optical Properties of Solids, (Academic Press, New York, 1972) and M.Dressel and G.Gruner, in Electrodynamics of Solids, (Cambridge University Press, 2002).
- <sup>19</sup> N.P.Ong and J.W.Brill, Phys.Rev.B 18, 5265 (1978) and N.P.Ong, Phys.Rev.B 18, 5272 (1978).
- <sup>20</sup> M.J.Rice et al., Phys.Rev.Lett. 37, 36 (1976).
- <sup>21</sup> L.Degorgi et al., Phys.Rev.B 44, 7808 (1991).
- <sup>22</sup> Different fitting procedures with variable number of fitting components were considered but yielded equivalent results. The temperature dependence of the extracted parameters and above all the redistribution of spectral weight unambiguously converge to a unique trend.
- <sup>23</sup> S.V.Dordevic et al., Eur.Phys.J.B 33, 15 (2003).
- <sup>24</sup> L.B.Ioffe and A.J.Millis, Science 285, 1241 (1999).
- <sup>25</sup> Because of the remaining Fermi surface and Dirac weight the CDW single particle excitations should be correctly named as pseudogaps. For simplicity we call them CDW gaps.
- <sup>26</sup> A.Schwartz et al., Phys.Rev.B 52, 5643 (1995).

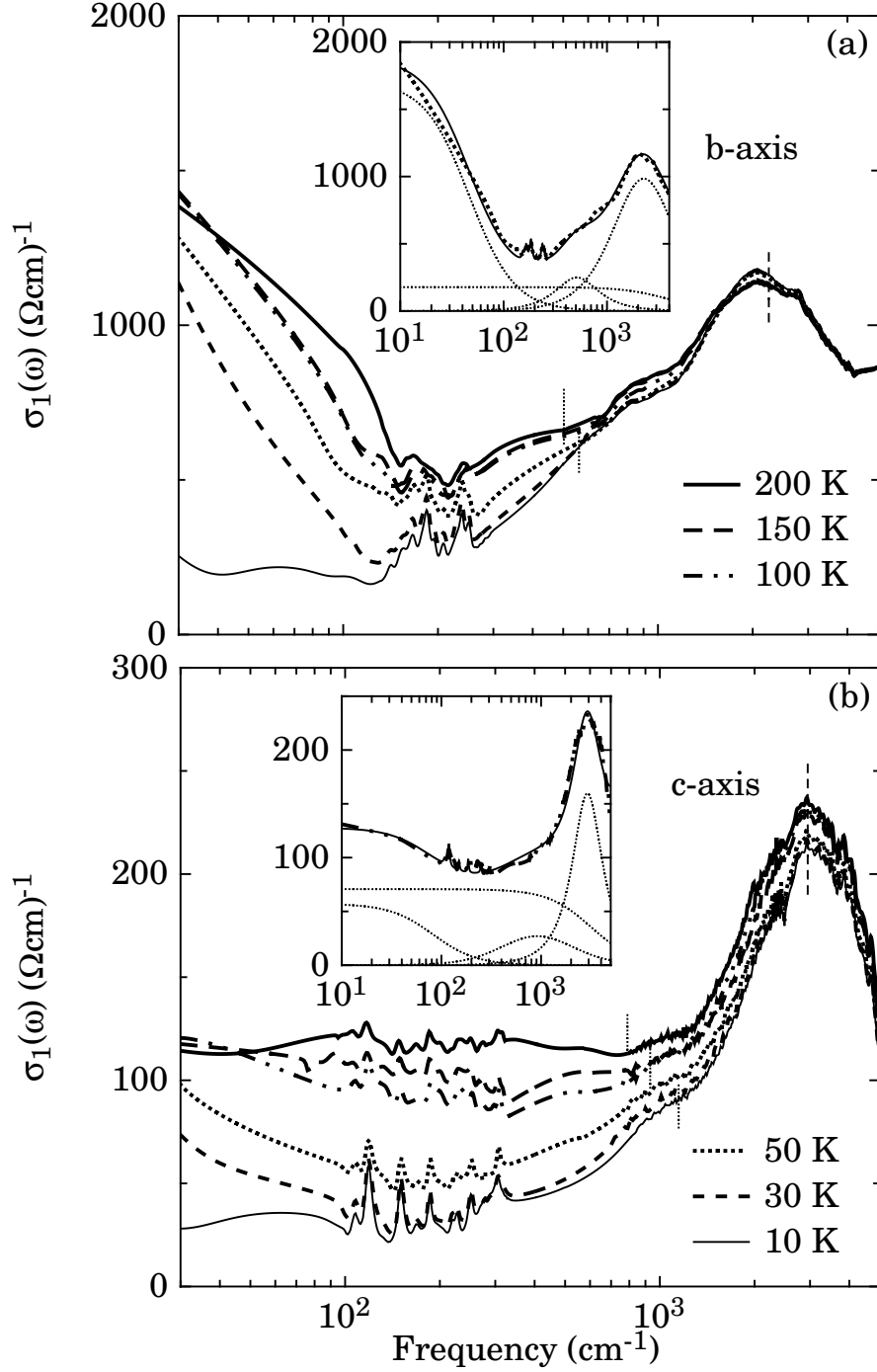


FIG. 2: Real part  $\sigma_1(\omega)$  of the optical conductivity above  $30 \text{ cm}^{-1}$  as a function of temperature along (a) the chain b-axis and (b) the transverse c-axis. The frequencies of the harmonic oscillators used to fit the two mid-infrared absorptions (see text) are indicated by thin dotted and dashed lines for the broad shoulder and the peak feature in  $\sigma_1(\omega)$ , respectively. The insets show the data at 50 K (b-axis) and 100 K (c-axis) with the total fit and its components.

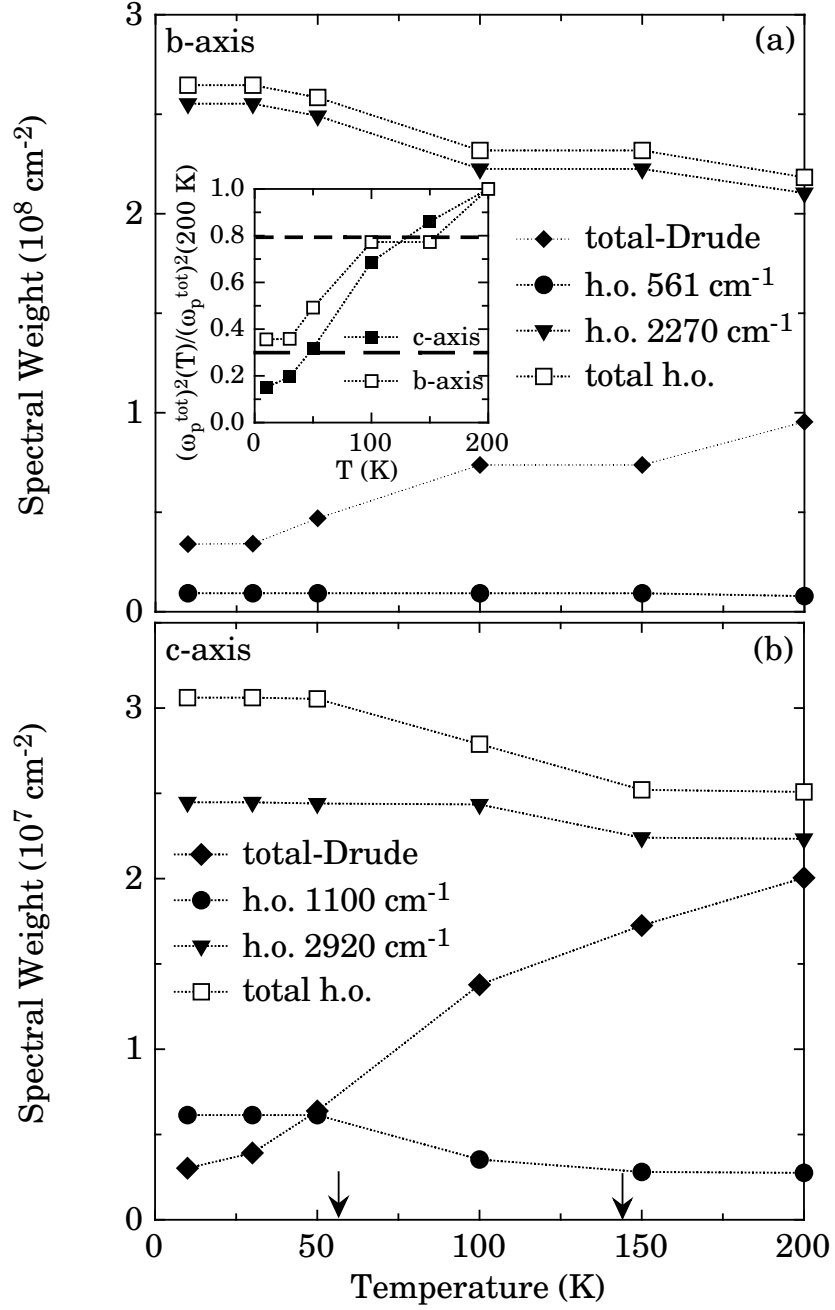


FIG. 3: Temperature dependence of the total spectral weight of the Drude terms and of the mid-infrared Lorentz harmonic oscillators, as well as of the spectral weights for the individual harmonic oscillators (a) along the b-axis and (b) along the transverse c-axis. The CDW transition temperatures are indicated by arrows. The inset in (a) shows the normalized change of the total Drude weight  $(\omega_p^{\text{tot}})^2$  with temperature, attributed to the gapping of the Fermi surface, for both axes. The dashed horizontal lines indicate the percentage of the Fermi surface which survives well below each of the two CDW transitions as determined by magnetotransport measurements<sup>6</sup>.